JOC The Journal of Organic Chemistry

ARTICLE

pubs.acs.org/joc

Stereolability of Dihydroartemisinin, an Antimalarial Drug: A Comprehensive Thermodynamic Investigation. Part 1†

Walter Cabri,[‡] Ilaria D'Acquarica,[§] Patrizia Simone,[§] Marta Di Iorio,[§] Michela Di Mattia,[‡] Francesco Gasparrini,*[,§] Fabrizio Giorgi,[‡] Andrea Mazzanti,[†] Marco Pierini,*[,§] Marco Quaglia,[‡] and Claudio Villani[§]

[‡]Analytical Development, R&D Department, sigma-tau S.p.A., Via Pontina km 30.400, 00040 Pomezia, Italy

[§]Dipartimento di Chimica e Tecnologie del Farmaco, Sapienza Università di Roma, P. le Aldo Moro 5, 00185 Roma, Italy

[†]Dipartimento di Chimica Organica "A. Mangini", Università di Bologna, Italy

Supporting Information

ABSTRACT: Artemisinin (Qinghaosu, **1**) is a sesquiterpene lactone endoperoxide isolated from *Artemisia annua* L. that Chinese herbalists have traditionally used to treat malaria. Reduction of artemisinin by $NaBH_4$ produced dihydroartemisinin (DHA, **2**) and yielded a new stereochemically labile center at C-10, which in turn provided two lactol hemiacetal interconverting epimers, namely, **2α** and **2β**. With the aim of fully investigating the thermodynamics of interconversion, we gathered the relative abundance of the two epimers within a wide variety of solvents and rationalized the results by linear solvation energy relationships (LSER) analysis. Beside the difference in polarity, the better stabilization of **2α** in polar solvents was found to be significantly related to its greater acidity with respect to **2β**, which was estimated by two independent theoretical approaches based on molecular modeling calculations and empirical data, and supported by ^{1}H NMR measurements. On the contrary, differential effects of cavitational energy have been highlighted as interactions strongly responsible for the small values of equilibrium constant measured for the $\beta \leftrightarrows \alpha$ process in the less polar media. Determination of forward and backward epimerization rate constants in seven media, clearly differing in both permittivity and capacity to be H-bond donors, indicated that, in the spontaneous process, the transition state of the rate-limiting step develops a significant degree of anionic character, as typically happens in the base-catalyzed breakdown of hemiacetals.

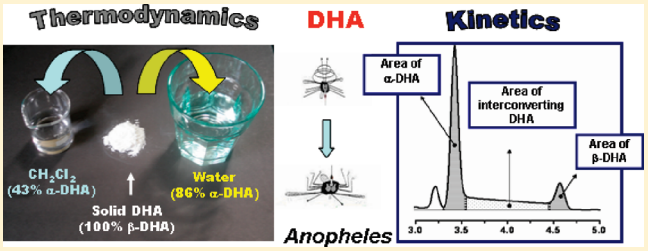

In the scenario opened by the threat posed by drug-resistant malaria, new antimalaria drugs, also effective against resistant parasites, are urgently needed, because mortality, currently estimated at up to three million people per year, has enormously risen in recent years.[1] Artemisinin (Qinghaosu, **1**, Chart 1) is a sesquiterpene lactone endoperoxide isolated from *Artemisia annua* L. that Chinese herbalists have traditionally used to treat malaria.[2] The combination of artemisinin derivatives with other effective antimalarial medicines (artemisinin-based combination therapies or ACTs) is currently the most effective treatment for *falciparum* malaria, the most lethal form of the disease.[3] Since its identification in the 1970s, artemisinin as well as semisynthetic derivatives[4] and synthetic trioxanes[5] have been utilized in therapy. Reduction of **1** by sodium borohydride[6] produced dihydroartemisinin (DHA, **2**, Chart 1), which is also its main metabolite and provides improved antimalarial potency.[5,7,8] Conversion of the lactone carbonyl group at C-10 of **1** into the hydroxyl (hemiacetal) group in **2** yielded a new stereochemically labile center in the molecule, which in turn provided two lactol hemiacetal epimers, namely, **2α** and **2β** (see Scheme 1). The α-epimer bears the hydroxyl group in the equatorial position (absolute stereochemistry at C-10 is *R*), and the β-epimer possesses an axial hydroxyl group.[9] Although **2** has a chairlike pyranose ring, such a nomenclature is the reverse of that normally used for designating the stereochemistry of sugars and glycosides, in which, for example, D-glucopyranose possesses an axial hydroxyl group.[10] Bulk solid **2** consists of the β-epimer, as illustrated by an X-ray crystallographic study on crystalline **2**.[11] Dissolution of vacuum-dried, bulk solid **2** in $CDCl_3$ provides a solution consisting exclusively of **2β**, which equilibrates to an approximately 1:1 mixture of **2α** and **2β** within 10 h.[11,12] The rate and extent of interconversion in solution is solvent-dependent: in nonpolar solvents such as CD_2Cl_2, the equilibrium ratio of **2α**/**2β** is 1:1.35, reaching values of 2:1 in methanol and acetone and 3:1 in dimethylsulfoxide,[12,13] according to the increased solvent polarity. In hydro-organic solvents, a 4.5:1 equilibrium ratio for **2α**/**2β** was reached after at least 18 h upon dissolution in 50% (v/v) ethanol in water at 4 °C.[14] HPLC determinations of the **2α**/**2β** ratio showed that a stable value (3.3:1) is achieved after 10−12 h in mobile phases comprising 50% (v/v) acetonitrile in 0.1 M acetate buffer (pH 4.8).[15,16] The **2α**/**2β** ratio was determined in vivo as well, in a study aimed also to obtain

Received: December 2, 2010
Published: February 22, 2011

Chart 1. Chemical Structures of Artemisinin (1) and Dihydroartemisinin (DHA, 2)

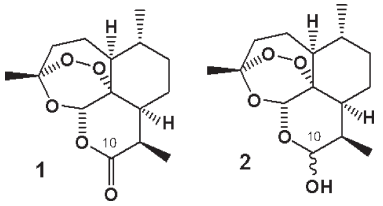

Scheme 1. Epimers of Dihydroartemisinin (DHA)

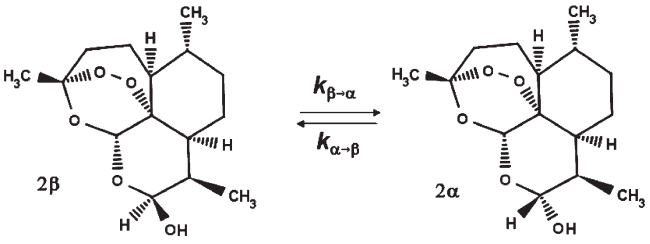

the protein binding of DHA: a preferential existence of the α-DHA epimer (**2α**/**2β** ratio of about 6:1) was assayed by HPLC with radiochromatographic detection in patients with malaria infection.[17]

Computational studies, performed with AM1 and PM3 semiempirical methods, showed that the DHA epimers have very close heats of formation, i.e., have similar thermodynamic stabilities.[10,12] It has also been found that acylations where the hydroxyl group of **2** acts as the nucleophile exclusively yield the α-acyl derivatives for kinetic reasons. The biological implication of such a process is the observation that phase II glucuronidation of **2** exclusively provides the α-DHA-β-glucuronide.[18,19]

Thus, a deeper understanding of the kinetic, thermodynamic, and mechanistic features of the **2α**/**2β** equilibration, including their stereochemical implications, may have great importance in the investigation of the mechanism of action and/or toxicity of the drug at molecular level. This paper deals with the thermodynamics of the $\beta \leftrightarrows \alpha$ interconversion, which has been studied to elucidate the molecular factors responsible for the change of the relative epimers abundance as a consequence of a solvent change. Convincing rationalization of the results has been obtained by a synergic integration of experimental and theoretical data.

RESULTS AND DISCUSSION

It has been found that the relative abundance of the **2α** and **2β** epimers is markedly influenced by the solvent, with the molar ratio [α]/[β] (i.e., the equilibrium constant $K_{\alpha/\beta}$ of the $\beta \leftrightarrows \alpha$ process; see Scheme 1) increasing with the polarity of the medium.[12,13] Such a behavior may find a first explanation in the greater dipolarity of the **2α** configuration, as predicted in terms of dipole moments by quantistic calculations in the gas phase and water at both semiempirical and DFT levels (see Table 1S of Supporting Information). However, to gain insight into the main solute−solvent interactions responsible for the differential solvation of the two epimers, we decided to carry out an in depth linear solvation energy relationships (LSER) analysis.

Effect of the Solvent on the Equilibrium Position. A significant number of $K_{\alpha/\beta}$ equilibrium constants at 25 °C, specifically measured by both NP-HPLC and RP-HPLC (for details see Experimental Section) in different solvents (23 items) or available from the literature (2 items),[12] were selected to perform the LSER statistical study (see Table 1). The solvents, absolute or as a mixture, were chosen to provide a wide typology of solute−solvent interactions, ranging from specific and aspecific coulombian interactions to dispersive forces. The explored permittivity range relative to vacuum was very wide (from 80.2 to 2.3), and among the selected solvents, 14 were made protic by the presence of water and/or alcohols. A quite regular permittivity distribution in the considered range was achieved by preparing suitable binary mixtures. As it is well-known, LSER analysis is based on the performance of a linear regression of a set of multiparameter equations, each of which can be expressed by the general formula

$$ {}^{x}\Delta G^{\circ} = {}^{gas}\Delta G^{\circ} + \sum f_i D_i = {}^{gas}\Delta G^{\circ} + {}^{x}\Delta G^{\circ solv} \qquad (1) $$

where ${}^{x}\Delta G^{\circ}$ is the change of standard free energy (ΔG°) relative to the considered process in solvent x, ${}^{gas}\Delta G^{\circ}$ is the constant obtained by regression expressing ΔG° in absence of solvent, D_i represents the generic i selected descriptor of solvation interactions, and f_i corresponds to its regression coefficient.

Descriptors D_i are able to selectively monitor the ability of a solvent to interact with solute molecules by noncovalent interactions. The role played by each type of interaction associated to the generic descriptor D_i is quantitatively expressed by the calculated value of the corresponding coefficient f_i. To analyze the differential solvation of the **2α** and **2β** epimers, we selected the six following D_i descriptors of solvent effects to be inserted into eq 1, where according to the monitored $\beta \leftrightarrows \alpha$ equilibrium ${}^{x}\Delta G^{\circ}$ corresponds to ${}^{x}\Delta G^{\circ}{}_{\alpha/\beta}$: the permittivity ($\varepsilon$) and cohesive pressure (δ^2) of the solvent, and the four solvatochromic parameters ET_{30}, T_N, α (hereafter denoted as α_d), and β (hereafter denoted as β_d).[20] These six descriptors, kept together, may conveniently monitor different and complementary interactions/effects arising between solute and solvent molecules, i.e., the capacity of electrostatic shielding of atomic charges (ε), the cavitational energy needed to host the solute molecules inside the solvent (δ^2), the electrostatic forces that, in general, may be established in both specific and aspecific ways, also including the dispersive ones (ET_{30} and T_N), the solvent lone pair donor capacity (β_d), and the solvent lone pair acceptor capacity (α_d). Numerous linear combinations of the cited descriptors, from 2 to 6 of them, have been considered, aimed at better understanding which parameters are really crucial in the whole solvation process, and dissecting the quantitative contribution coming from each relevant kind of interaction. Afterward, the regression results have been analyzed according to statistics (*F*-test and *t* test) to reasonably exclude casualness (index *F*) and to quantify the statistical weight of each used descriptor (index *T* and factor t_i). A selection of equations endowed with all statistically significant descriptors has been summarized in Table 2, while the composition of the considered multiparameter equations, as well as the statistical results related to their use, have been extensively collected in Table 2S of Supporting Information. A detailed discussion of the established efficacy of each descriptor in describing the solvent effect when it is employed in a suitable combination with the others is given in Supporting Information.

Although the best statistically significant correlation was achieved by combination of all the six descriptors (entry 19 in

Table 1. Thermodynamic Ratios ($K_{\alpha/\beta}$) of 2α and 2β as Function of Solvent at 25 °C and Values of Descriptors Used in the LSER Analysis

solvent	ε	ET_{30}	T_N	α_d	β_d	δ^2	$\Delta G^\circ_{\alpha/\beta}$[a]	$K_{\alpha/\beta}$
H_2O	80.2	63.1	0.62	1.170	0.470	552.3	−1.06	6.0
10/90 CH_3OH/H_2O	70.7	62.2	0.73	1.151	0.489	509.8	−1.08	6.2
10/90 CH_3CN/H_2O	69.4	61.5	0.73	1.072	0.463	499.2	−0.99	5.3
30/70 CH_3OH/H_2O	56.9	60.0	0.68	1.113	0.527	429.9	−0.94	4.9
30/70 CH_3CN/H_2O	56.0	58.4	0.66	0.876	0.449	401.0	−0.89	4.5
50/50 CH_3CN/H_2O	48.0	57.1	0.65	0.680	0.435	313.6	−0.78	3.7
50/50 CH_3OH/H_2O	47.3	58.3	0.62	1.075	0.565	356.8	−0.84	4.1
DMSO	46.7	45.1	1.00	0.000	0.760	167.2	−0.65	3.0[b]
70/30 CH_3CN/H_2O	42.8	56.8	0.58	0.484	0.421	237.0	−0.69	3.2
70/30 CH_3OH/H_2O	40.2	57.1	0.57	1.037	0.603	290.6	−0.72	3.4
90/10 CH_3CN/H_2O	39.0	54.6	0.53	0.288	0.407	171.0	−0.60	2.8
CH_3CN	37.5	45.6	0.49	0.190	0.400	142.1	−0.41	2.0
90/10 CH_3OH/H_2O	34.8	56.1	0.47	0.999	0.641	231.1	−0.63	2.9
CH_3OH	32.6	55.4	0.40	0.980	0.660	203.9	−0.56	2.6 (2.0) [b]
CH_3CH_2OH	24.6	51.9	0.37	0.860	0.750	166.9	−0.27	1.6
CH_2Cl_2	8.9	40.7	0.48	0.130	0.100	98.6	0.18	0.74[b]
THF	7.6	37.4	0.34	0.000	0.550	90.6	0.33	0.57
$CHCl_3$	4.8	39.1	0.43	0.200	0.100	84.8	0.02	0.97 (1.0) [b]
20/80 $C_6H_{12}/CHCl_3$	4.2	37.5	0.40	0.160	0.080	81.1	0.15	0.78
40/60 $C_6H_{12}/CHCl_3$	3.7	35.8	0.36	0.120	0.060	77.4	0.22	0.69
60/40 $C_6H_{12}/CHCl_3$	3.1	34.2	0.29	0.080	0.040	73.8	0.29	0.61
80/20 $C_6H_{12}/CHCl_3$	2.6	32.5	0.23	0.040	0.020	70.3	0.38	0.53
97/3 C_6H_{12}/CH_3CH_2OH	2.3	31.6	0.03	0.030	0.020	54.9	0.37	0.54

[a] kcal mol^{-1}. [b] Data available from ref.[12]

Table 2. Multiparameter Equations Employed in the LSER Analysis Endowed with All Statistically Significant Descriptors

entry	descriptors/t_i						T index	F index	R^2
1	ε 16.9						2.1	1.4×10^{-18}	0.932
2	ET_{30} 16.8						2.1	1.6×10^{-18}	0.931
3	T_N 6.1						2.1	1.0×10^{-9}	0.638
4	δ^2 9.2						2.1	3.2×10^{-13}	0.802
5	α_d 6.8						2.1	1.3×10^{-10}	0.686
6	β_d 4.5						2.1	2.5×10^{-7}	0.487
7	ET_{30} 5.1	ε 5.2					2.1	6.2×10^{-19}	0.971
8	α_d 2.3	ε 9.9					2.1	3.0×10^{-16}	0.947
9	T_N 4.6	ET_{30} 14.0					2.1	2.3×10^{-18}	0.967
10	β_d 3.8	δ^2 8.3					2.1	9.0×10^{-13}	0.885
11	β_d 2.1	α_d 4.5					2.1	7.0×10^{-9}	0.745
12	δ^2 6.2	T_N 3.5					2.1	2.0×10^{-12}	0.877
13	α_d 8.0	T_N 7.3					2.1	4.1×10^{-14}	0.914
14	β_d 2.3	T_N 4.0					2.1	2.8×10^{-8}	0.713
15	T_N 3.0	ET_{30} 6.4	ε 3.5				2.1	3.3×10^{-18}	0.980
16	α_d 3.7	T_N 2.9	ε 5.0				2.1	1.2×10^{-15}	0.963
17	α_d 6.1	δ^2 3.7	T_N 3.2	ε 7.1			2.1	3.6×10^{-16}	0.979
18	β_d 2.4	α_d 6.5	T_N 4.2	δ^2 4.6	ε 7.9		2.1	1.1×10^{-15}	0.984
19	β_d 2.5	α_d 3.0	T_N 4.0	δ^2 3.6	ET_{30} 2.6	ε 5.2	2.1	2.1×10^{-15}	0.989

Table 2), we decided to select the equation based on the five descriptors β_d, α_d, T_N, δ^2, and ε (entry 18 in Table 2), which indeed showed a good correlation ($R^2 = 0.98$) together with the minimum number of essential, highly specialized and unrelated parameters, widely significant according to the t test. In fact, although an equation solely based on the three descriptors T_N, ET_{30}, and ε of entry 15 would allow a good estimation of ${}^x\Delta G^\circ_{\alpha/\beta}$ values, these three parameters would not be able to efficiently dissect all the most relevant solute−solvent contributions to achieve the epimerization ratios. In particular, descriptors T_N and ET_{30} are not so strongly specialized and, above all, not so independent one to each other. Solvent contributions to ${}^x\Delta G^\circ_{\alpha/\beta}$

dx.doi.org/10.1021/jo102391s |J. Org. Chem. 2011, 76, 1751–1758

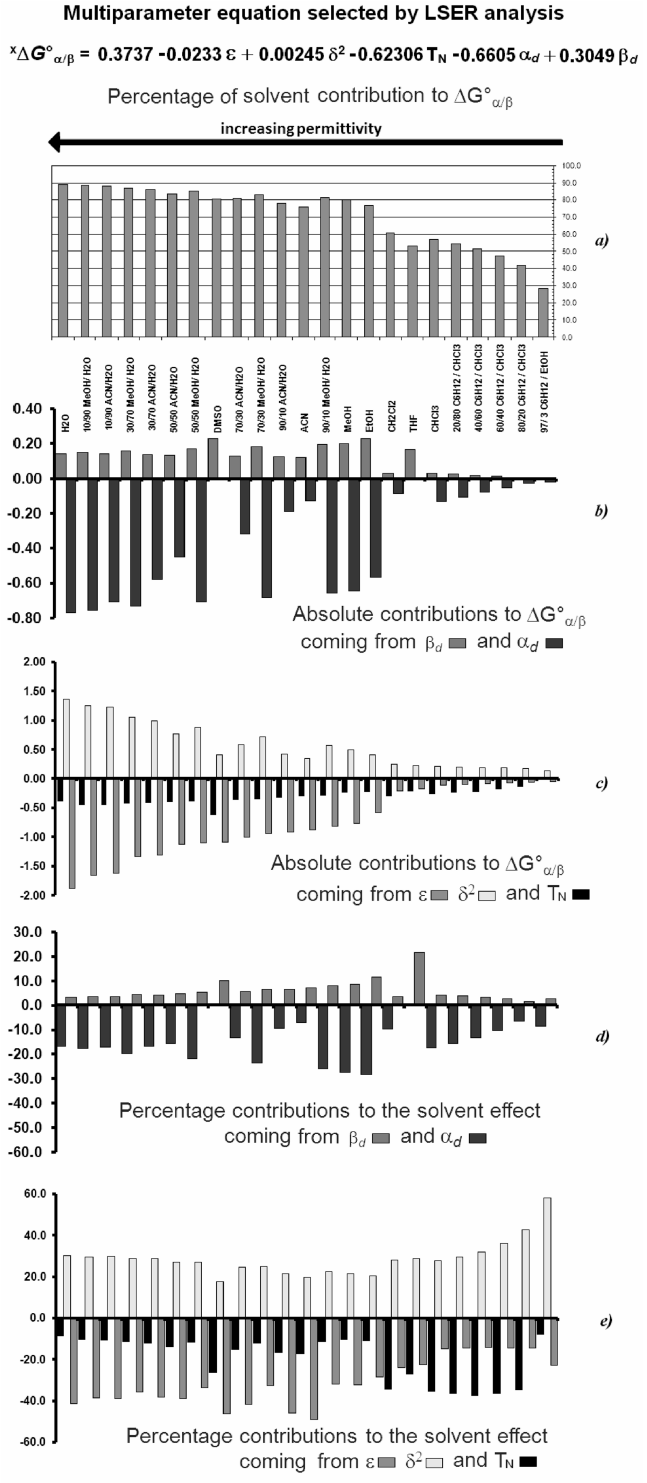

Figure 1. Bar plots of the absolute and relative solvent contributions to $\Delta G^{\circ}_{\alpha/\beta}$.

(i.e., the amount of energetic contribution $^{x}\Delta G^{\circ}_{\alpha/\beta}{}^{solv}$ that the solvent brings to $^{x}\Delta G^{\circ}_{\alpha/\beta}$) were accordingly calculated (see Table 3S of Supporting Information) and are schematically represented in Figure 1. Inspection of such data revealed that the solvent contribution governs the $^{x}\Delta G^{\circ}_{\alpha/\beta}$ (from 70% to 92% of the total) when permittivity ε becomes greater than about 9, irrespective of the protic or aprotic nature of the medium. For ε values in the 2.5−9 range, the contribution drops down to 50% and decreases further to 40% for solvents with polarity similar to that of *n*-hexane. Interestingly, in all the considered media, the LSER analysis suggested that the H-bonds donor capacity of solvent (α_d), the aspecific electrostatic (ε), and the dispersive interactions (T_N) favors the **2α** epimer, whereas H-bonds acceptor capacity of solvent (β_d) and the cavitational energy (δ^2) favors the **2*β*** epimer. In particular, this latter factor shows a greater effect in the less polar media (from 28% to 58% of the whole solvent effect on $^{x}\Delta G^{\circ}_{\alpha/\beta}$, in the 2−9 permittivity range), the same in which the experimental $^{x}\Delta G^{\circ}_{\alpha/\beta}$ values are found greater than zero (i.e., when $K_{\alpha/\beta} < 1$). A rational explanation of this behavior may be given by the theoretical calculation of the molar volumes of the two epimers, which yielded a larger value for **2α** ($\Delta V_{\alpha-\beta}$ = 1.4 cm^3/mol). This finding also suggests that the **2*β*** epimer may be better packed in the solid state than **2α**, as experimentally observed.[11] It was also found that the aspecific electrostatic interactions, monitored by ε, percentually play the most important role when permittivity is greater than 24 (ε > 24). This finding may be ascribed to the greater dipolar moment of **2α**, as predicted by quantistic calculations performed at both low and high level (see Table 1S of Supporting Information). The computed dipolar difference increases with the permittivity of the solvent ($\Delta\mu_{\alpha-\beta}$ = 1.37 debyes in the gas phase and $\Delta\mu_{\alpha-\beta}$ = 3.64 debyes in water), thus making the differential effect more relevant in media with larger ε values (Figure 1c). The dispersive forces, whose descriptor T_N has greater relevance for ε < 24, act in an almost complementary way. Thus, aspecific and dispersive solute−solvent interactions give a quite constant contribution to the $^{x}\Delta G^{\circ}_{\alpha/\beta}{}^{solv}$ in favor of **2α**, irrespective of the nature of the solvent (51% ± 9% is the calculated average value). On the contrary, contributions coming from H-bond interactions are percentually less important.

In addition, because the donor and acceptor capacity of the solvent has an opposite effect on $^{x}\Delta G^{\circ}_{\alpha/\beta}$, with the former prevailing over the latter, it resulted that the **2α** isomer was favored also by this kind of forces, especially in pure alcohols or in strongly alcoholic media (Figure 1d). Dimethyl sulfoxide (DMSO) and tetrahydrofuran (THF) clearly represent an exception to this trend, because they exclusively behave as H-bond acceptors, being aprotic solvents. Although small, the contribution to $^{x}\Delta G^{\circ}_{\alpha/\beta}{}^{solv}$ suggested by the β_d descriptor is however significant (an average contribution of 6% ± 4%), especially in THF (22%), DMSO (10%), and alcoholic media (up to 11% in ethanol). However, on the whole, the specific interactions monitored by a combination of α_d and β_d may influence $^{x}\Delta G^{\circ}_{\alpha/\beta}{}^{solv}$ for 21% ± 8%. This means that, in all the solvents, but preferentially in those with medium-high permittivity, the thermodynamic position of epimerization must be significantly affected by a different acidity of the hemiacetal hydroxyl groups of **2α** and **2*β***. Such an interesting indication prompted us to investigate the acidity of **2α** and **2*β*** epimers.

Acidity of 2α and 2*β* Epimers. At the beginning, we faced the problem of the nonsuitability of commercial computer software to calculate pK_a of stereoisomers, as in general they cannot take into account differences related only to the stereochemistry of the analyzed species. In fact, by use of the well-known packages ACD/pK_a[21a] and Marvin,[21b] we obtained the same value for both the epimers: 12.88 by ACD/pK_a and 12.23 by Marvin. For this reason, we decided to calculate the two pK_a values using the

dx.doi.org/10.1021/jo102391s |*J. Org. Chem.* 2011, 76, 1751–1758

Scheme 2. Derivation of eq 3 Used to Assess the Acidity of 2α and 2β

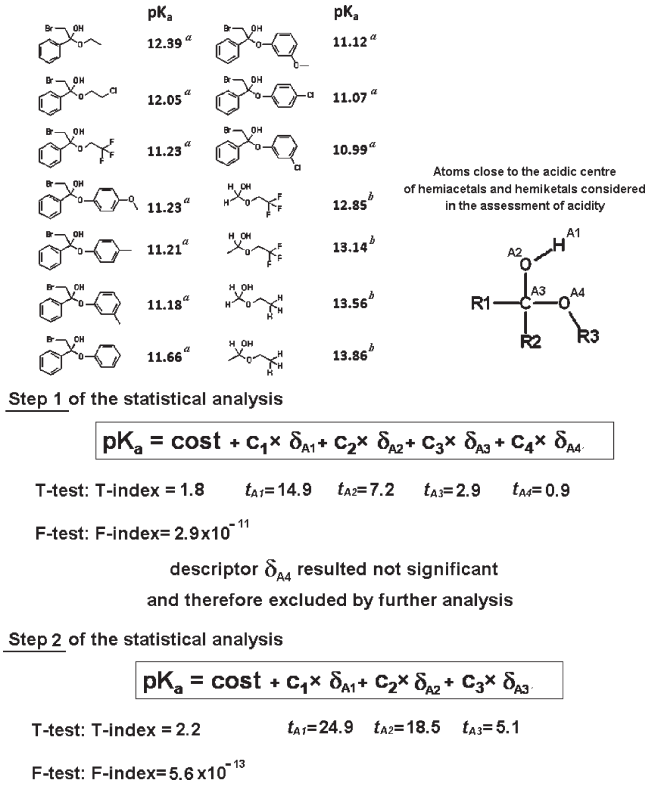

[a] See ref 23a. [b] See ref 23b.

multiparameter eq 2:

$$pK_a = C_0 + \sum C_i \times \delta_i \qquad (2)$$

containing, as molecular descriptors of acidity, the density charge values (δ_i).[22] These latter were calculated by an ab initio procedure (Hartree−Fock, basis set 3-21G(*)) on atoms close to the hydroxyl moiety of hemiacetals or hemiketals used as empirical references (see Scheme 2), and whose acidity values in water (pK_a) were available from the literature.[23]

Parameters C_0 and C_i have been optimized by linear regression analysis on a set of equations related to 14 (n = 14) pK_a data (Scheme 2). The statistical significance of each considered δ_i descriptor has been checked by t test, as well as the exclusion of casualness of the obtained results by F-test. After such analysis (for more details see the Experimental section) we obtained the following equation:

$$pK_a = -19.86 - 87.43 \times \delta_{A1} - 94.51 \times \delta_{A2} + 1.84 \times \delta_{A3} \qquad (3)$$

with n = 14, R^2 = 0.9950, and SD = 0.06. By inserting into eq 3 the density charge values calculated on the sensible A1, A2, and A3 atoms (as defined in Scheme 2) within the optimized structures of **2α** and **2β**, we assessed for these species the following acidities in water: pK_a = 12.49 ± 0.06 for **2α** and pK_a = 12.84 ± 0.06 for **2β** (see Figure 2), with a $\Delta pK_a^{\alpha-\beta}$ equal to −0.35 in favor of **2α**. This information is consistent with the more deshielded ^{1}H NMR signal observed for the hemiacetal hydroxyl hydrogen of **2α** in both d_6-DMSO ($\Delta\delta_{\alpha-\beta}$ = 0.14 ppm) and CD_3CN ($\Delta\delta_{\alpha-\beta}$ = 0.16 ppm)[24]

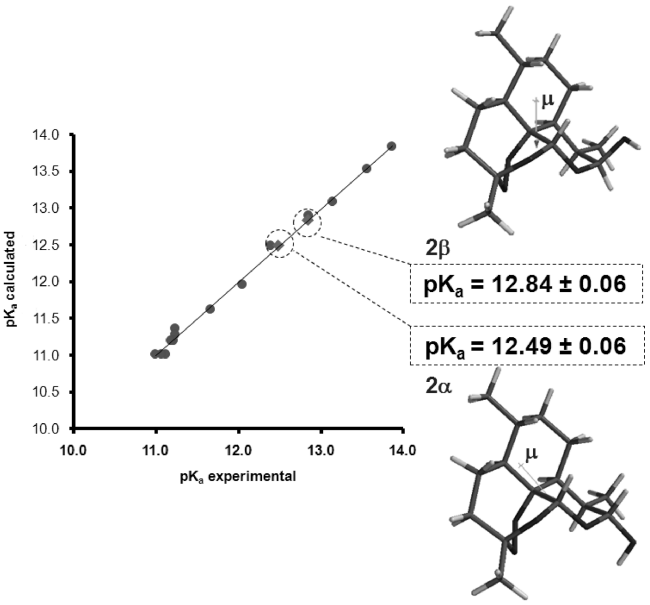

Figure 2. Plot of some hemiacetal and hemiketal pK_a values available from the literature[23] versus the corresponding calculated according to eq 3 (●). Estimated acidities of **2α** and **2β** are shown by filled squares (◆) on the correlation straight line.

and supplies an interesting interpretation of the results found by LSER analysis (full NMR spectra and NOE assignment of **2α** and **2β** are given in Supporting Information). The ability of lone pair donor solvents to favor **2β** suggests that the transient adducts generated by H-bond donation from **2** to solvent molecules can be considered as activated species toward an easier epimerization. Consequently, such an effect, typical of a base-catalysis (*vide infra*), should plausibly favor a more marked isomerization of the more acidic **2α** epimer. On the contrary, solvent molecules acting as H-bond donors toward the hemiacetal hydroxyl group should proportionally inhibit the quoted base-catalyzed epimerization mechanism by entropic reasons and thus favor the more acidic **2α** epimer.

Because of the conceptual relevance of this result, we searched a further confirmation of the differential acidity of the epimers by performing the estimation through an independent approach, based on the thermodynamic cycle reported in Scheme 3. As it can be seen, both ionization and epimerization equilibria were considered, in particular ionization of both **2α** and **2β** (K_i^{α} and K_i^{β} being the respective ionization constants) and epimerization either between **2α** and **2β** or their conjugate bases $\mathbf{2\alpha}^-$ and $\mathbf{2\beta}^-$, whose equilibrium constants were expressed by the symbols $K_{\alpha/\beta}$ and $K^-_{\alpha/\beta}$, respectively.

By simple algebraic steps, the relationships between constants K_i^{α}, K_i^{β}, $K_{\alpha/\beta}$, and $K^-_{\alpha/\beta}$ may be conveniently expressed by eq 4, which in turn may also be rewritten in the more convenient eqs 5 and 6:

$$K_i^{\beta}/K_i^{\alpha} = K_{\alpha/\beta}/K^-_{\alpha/\beta} \qquad (4)$$

$$-\log(K_{\alpha/\beta}) = -\log(K^-_{\alpha/\beta}) - \log(K_i^{\beta}) + \log(K_i^{\alpha}) \qquad (5)$$

$$\Delta pK_i^{\alpha-\beta} = \log(K_{\alpha/\beta}) - \log(K^-_{\alpha/\beta}) \qquad (6)$$

According to eq 6, $\Delta pK_i^{\alpha-\beta}$ in a given solvent (corresponding to $\Delta pK_a^{\alpha-\beta}$ in water) can be easily obtained by the logarithm

dx.doi.org/10.1021/jo102391s |J. Org. Chem. 2011, 76, 1751–1758

Scheme 3. Thermodynamic Cycle Involving 2α and 2*β* Epimers and Their Conjugated Bases

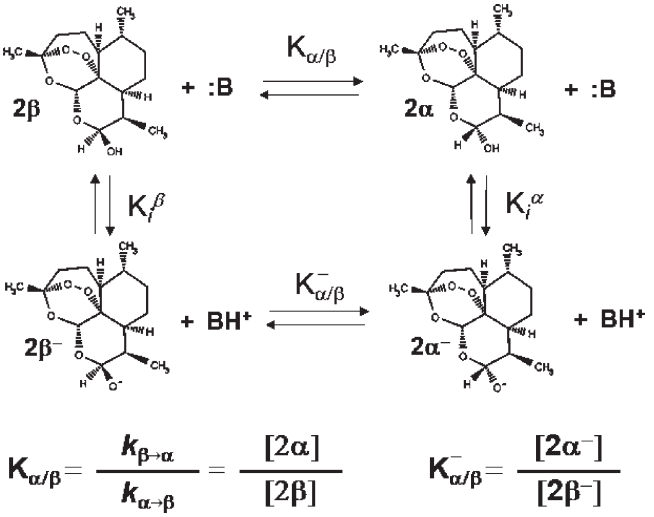

Scheme 4. Base-Catalyzed Breakdown of Hemiacetal 2α and 2*β*

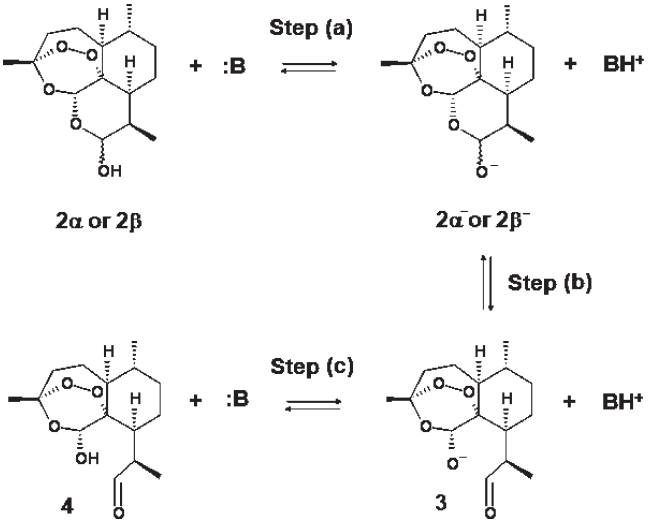

difference between equilibrium constants $K_{\alpha/\beta}$ and $K^-_{\alpha/\beta}$, both assessed in the same medium by molecular modeling calculations. We obtained the required epimerization constants $K_{\alpha/\beta}$ and $K^-_{\alpha/\beta}$ by the related energetic differences between **2α** and **2*β*** and between **2α**$^-$ and **2*β***$^-$, respectively, optimizing the structure of such species through DFT calculations at two different levels of accuracy (see Table 1S of Supporting Information) and taking into account the solvent effect in three media endowed with very different permittivities: *n*-hexane (ε = 1.90), acetonitrile (ε = 37.5), and water (ε = 80.2). The aptitude of such approach to properly assess the experimental data was checked by calculating the ratios between experimental and predicted $K_{\alpha/\beta}$ constants in the aforementioned solvents. As may be seen, apart from a constant factor of 3.6 ± 0.3 (3.0 at the higher level of calculus), calculations reproduced with good accuracy the relative abundance of the epimers. Because an error factor of similar extent was also expected for calculation of the $K^-_{\alpha/\beta}$ constants, it was reasonable to predict they may roughly cancel one another in eq 6, thus showing that the approach was suitable for the purpose. Notably, the result obtained at the higher level of calculus in water (basis set: GGA-BLYP/QZ4P, large core, water solvation: COSMO, SES algorithm) indicated an acidity difference ${}^{W}\Delta pK_i^{\alpha-\beta}$ between **2α** and **2*β*** equal to −1.1 pK_a units (−1.6 pK_a units from the lowest level of calculus), reasonably close to that assessed by eq 3 (−0.4 pK_a units). In addition, the calculations performed at the lower level (basis set: GGA-BLYP/DZP, medium core, solvation: COSMO, SES algorithm) showed that the differential acidity of the two epimers should increase with the apolarity of the solvent (${}^{HE}\Delta pK_i^{\alpha-\beta}$ = −2.2, ${}^{ACN}\Delta pK_i^{\alpha-\beta}$ = −1.8, ${}^{W}\Delta pK_i^{\alpha-\beta}$ = −1.6, the superscripts HE, ACN, and W referring to *n*-hexane, acetonitrile, and water).

Hemiacetal Ring-Opening Process. To gather insights into the nature of the spontaneous hemiacetal ring opening of **2**, we performed a kinetic study by analyzing the effects that a change of solvent has on the epimerization rate constants of **2**. For this purpose, we monitored the **2*β*** ⇆ **2α** epimerization in seven solvent systems, endowed with significantly different permittivity (ε) and capacity to be H-bond donors. Three of them were made of absolute solvents (tetrahydrofuran, acetonitrile, and methanol), while the others were prepared as either binary or ternary aqueous mixtures. In the pure media, the measurements were performed by classic batchwise approach, using HPLC with UV detection (see the Experimental Section). In the composite solvents, the rate constants were obtained by dynamic HPLC (DHPLC),[25] the system solvent being the mobile phase itself. Simulations of experimental dynamic chromatograms were performed by using the Auto DHPLC y2k lab-made computer program.[26] The relative experimental and superimposed simulated chromatograms are collected in Figure 1S of Supporting Information. Inspection of the results collected in Table 4S of Supporting Information clearly showed that faster interconversions occurred in more polar media. However, comparison of the rate constants also indicated that the effect can be more ascribed to the protic nature of some of the solvents than to permittivity differences. In fact, for the couple of pure solvents MeOH/ACN, the rate constants ratio was found greater than 10^2 in favor of MeOH, irrespective of the similar permittivities, whereas for the THF/ACN couple the rate constants were close to each other, even if their permittivities differ by about 30 units. As a further confirmation, similar rate constants were found for the four protic hydro-organic media, although the greatest difference was observed between those featuring the same permittivity. This means that, in the spontaneous process, the transition state of the rate-limiting step develops a significant degree of anionic character, which in turn may be efficiently stabilized by H-bonds formation with molecules of protic solvents. Notably, this is what typically happens in the base-catalyzed breakdown of hemiacetals,[23] according to the mechanism depicted in Scheme 4 and in rational agreement with what was found by LSER analysis (*vide supra*). Van't Hoff analysis of the free energy activation barriers for the **2*β*** to **2α** and backward interconversions in the mixed protic solvents of Table 4S of Supporting Information showed small temperature dependences, with negative $\Delta S^{\ddagger}$ never smaller than −20 entropic units (eu).

■ CONCLUSIONS

The present study was conceived to achieve a deeper understanding of the thermodynamics of the **2α**/**2*β*** equilibration, by both experimental and theoretical approaches. By LSER analysis,

dx.doi.org/10.1021/jo102391s |*J. Org. Chem.* 2011, 76, 1751–1758

it was elucidated that the ratio of the **2α** and **2β** epimers in different media is strictly related to at least three properties of the solvent: (i) the permittivity, which modulates the formation of aspecific electrostatic solute−solvent interactions, (ii) the cohesive pressure, which influences the cavitational energy needed to host the solute inside the solvent, and (iii) the capacity to establish H-bonds with the solute. In particular, a greater value of permittivity and a better aptitude to be a good H-bond donor lead to a more effective stabilization of **2α**, which was assessed by theoretical calculations to be more polar and more acid than **2β**. On the contrary, a better propensity of the solvent to be a good H-bond acceptor and greater values of cohesive pressure should play in favor of **2β**, whose molar volume was estimated to be smaller than that of **2α**. Thus, protic media and/or media endowed with suitably high permittivity (e.g., greater than ∼9) yield epimerization equilibria with $K_{\alpha/\beta}$ constants greater than 1. On the other hand, the same process appeared to be kinetically promoted by protic solvents but only marginally affected by changes of permittivity. This clearly indicates that, in the spontaneous epimerization, the transition state of the rate-limiting step develops a significant degree of anionic character, as typically happens in the base-catalyzed breakdown of hemiacetals. Interestingly, this latter finding closely supports the relationship highlighted by LSER analysis that correlates the greater acidity of **2α** with its more marked tendency to epimerize with respect to **2β**, thus leading to an increase of the $K_{\alpha/\beta}$ constant with the solvent proticity. To complete the investigation, kinetic studies have also been performed on the **2β** ⇆ **2α** process. The effects of solvent, pH, ionic strength, and temperature on the rate of the event, as well as of unattended details on the involved mechanism of epimerization have been elucidated, and they will be the subject of part 2.

EXPERIMENTAL SECTION

Chromatography. Analytical liquid chromatography was performed using an HPLC separation module coupled with a Photodiode Array Detector. Chromatographic data were collected and processed using Empower2 software. Variable temperature HPLC (DHPLC) was performed by using a lab-made thermally insulated container cooled by the expansion of liquid carbon dioxide (CO_2). Flow of liquid CO_2 and column temperature were regulated by a solenoid valve, thermocouple, and electric controller. Temperature variations after thermal equilibration were within ±0.2 °C.

Normal-phase HPLC for classic batch-wise approach was performed on a Reprosil Si 120, 3 μm (150 mm × 4.6 mm i.d.) column, with a mobile phase made up of *n*-hexane/ethanol 97:3 (v/v), delivered at 1.0 mL min^{-1}, and UV detection at 214 nm (T = 25 °C). Reversed-phase HPLC was performed on a C18 Symmetry, 3.5 μm (100 mm × 4.6 mm i.d.) column, with a mobile phase composed of water/acetonitrile/methanol 55:35:10 (v/v/v) buffered to apparent pH 5.6 using 10 mM sodium phosphate, delivered at 1.0 mL min^{-1}, and UV detection at 214 nm (T = 5 °C).

All the DHPLC experiments were performed on a C18 Symmetry, 3.5 μm (75 mm × 4.6 mm i.d.) column, with different binary and ternary hydro-organic mobile phases delivered at 1.0 mL min^{-1} and UV detection at 214 nm.

Simulation of Dynamic Chromatograms. Simulations of experimental dynamic chromatograms were performed by using the Auto DHPLC y2k lab-made computer program,[26] which implements both stochastic and theoretical plate models.[25] The developed algorithm may take into account all the types of first-order interconversions, i.e., enantiomerizations as well as diastereomerizations or constitutional isomerizations (e.g., pseudo-first-order tautomerizations), as well as tailing effects. The effective functionality of the program was widely validated on a consistent number of first-order isomerizations (both enantiomerization and non-enantiomerization) by comparing DHPLC results with those obtained by DNMR technique[26a−26d] or the batchwise approach.[26e] In the present paper, all simulations were performed employing the stochastic model and taking tailing effects into consideration. In all cases, the rate constants in mobile phase were properly set in order to obtain an epimers ratio consistent with the thermodynamic $K_{\alpha/\beta}$ ratio experimentally measured in the same media by ^{1}H NMR by means of the DPFGSE solvent suppression sequence, as reported elsewhere.[27]

NMR Measurements. NMR spectra were recorded at T = 25 °C on a 600 MHz spectrometer equipped with a triple resonance indirect probe, and CD_3CN was used as the solvent. The standard pulse sequence and phase cycling were used for gradient-enhanced COSY, HSQC, and HMBC spectra. NOE spectra were acquired by means of the DPFGSE-NOE sequence,[28] using a mixing time of 3.0 s and two "rSNOB" 50 Hz-wide selective pulses. Data acquisition, Fourier transformation, and spectra elaboration were performed using the software VNMRJ, 1.1D.

LSER Analyses. Both linear regression analyses and *F*-test and *t* test statistical evaluations were performed by the dedicated functions implemented in the Microsoft Office Excel 2003 program. Probability related to the *t*-Student distribution in the *t* test was set to 0.05.

Molecular Modeling Calculations. All molecular modeling calculations were performed on a PC equipped with Intel Pentium 4, CPU 3.40 GHz, 2 GB of RAM and OS Windows 2000 Professional. Geometries of **2α**, **2β**, **2α**$^-$, and **2β**$^-$, as well as of hemiacetals and hemiketals used to obtain eq 3 were optimized at the SCF level by the semiempirical and Hartree−Fock/3-21G(*) methods implemented within the computer program SPARTAN 04 (Wave Function Inc., 18401 Von Karman Avenue, Suite 370, Irvine, CA 92612, USA). With the same package were evaluated the relative hydration energies by the SM5.4/A solvation model. Geometries of **2α**, **2β**, **2α**$^-$, and **2β**$^-$ were further optimized at the SCF level by DFT calculations run with the Amsterdam density functional (ADF) package v. 2007.01 at two different levels of precision. Calculations at the lower level were carried out by the GGA-BLYP method with DZP medium core basis set, whereas the GGA-BLYP method with QZ4P large core basis set was used for calculations at the higher level (only on **2α**, **2β**, **2α**$^-$, and **2β**$^-$). All of the relative solvation energies in *n*-hexane, acetonitrile, and water were computed with the same program by the conductor like screening model (COSMO), with the cavity defined according to the solvent excluding surface (SES) algorithm. Approximate assessments of molar volumes for **2α** and **2β** were based on the estimation of the respective molecular volumes performed by both SPARTAN 04 and the QSAR Properties calculator implemented in the computer program HyperChem Professional release 7.5.

ASSOCIATED CONTENT

Supporting Information. Calculated properties of the optimized structures of **2α** and **2β** and of their conjugate bases **2α**$^-$ and **2β**$^-$. Multiparameter equations employed in the LSER analysis. Energetic contributions to $^*\Delta G^\circ_{\alpha/\beta}$. Pseudo-first-order epimerization rate constants measured at different temperatures and relative activation enthalpies and entropies. Superimposed experimental and simulated dynamic chromatograms of **2** dissolved in unbuffered solutions. Full NMR assignments of **2**. Assignment of the configuration at C-10 of **2**. Cartesian coordinates of **2α**, **2β**, **2α**$^-$, and **2β**$^-$. Cartesian coordinates and descriptors of acidity of hemiacetals and hemiketals employed in the assessment of pK_a values for **2α** and **2β**. This material is available free of charge via the Internet at http://pubs.acs.org.

AUTHOR INFORMATION

Corresponding Author

*E-mail: francesco.gasparrini@uniroma1.it; marco.pierini@uniroma1.it.

ACKNOWLEDGMENT

We are grateful for financial support from FIRB, Research program: Ricerca e Sviluppo del Farmaco (CHEM-PROFARMA-NET), grant no. RBPR05NWWC_003.

DEDICATION

†This paper is dedicated to the memory of Paolo Carminati, who passed away on April 2, 2010.

REFERENCES

(1) *Guidelines for the Treatment of Malaria*; World Health Organization: Geneva, 2009.

(2) (a) Klayman, D. L. *Science* **1985**, *228*, 1049–1055. (b) Chaturvedi, D.; Goswami, A.; Saikia, P. P.; Barua, N. C.; Rao, P. G. *Chem. Soc. Rev.* **2010**, *39*, 435–454.

(3) Ashley, E. A.; White, N. J. *Curr. Opin. Infect. Dis.* **2005**, *18*, 531–536.

(4) O'Neill, P. M. *Expert Opin. Invest. Drugs* **2005**, *14*, 1117–1128.

(5) (a) O'Neill, P. M.; Posner, G. H. *J. Med. Chem.* **2004**, *47*, 2945–2964. (b) Bez, G.; Kalita, B.; Sarmah, P.; Barua, N. C.; Dutta, D. K. *Curr. Org. Chem.* **2003**, *7*, 1231–1255.

(6) Li, Y.; Yu, P.-L.; Chen, Y.-X.; Li, L.-Q.; Gai, Y.-Z.; Wang, D.-S.; Zheng, Y.-P. *Chin. Sci. Bull.* **1979**, *24*, 667–669.

(7) Posner, G. H.; Paik, I.-H.; Chang, W.; Borstnik, K.; Sinishtaj, S.; Rosenthal, A. S.; Shapiro, T. A. *J. Med. Chem.* **2007**, *50*, 2516–2519.

(8) Li, Q. G.; Peggins, J. O.; Fleckenstein, L. L.; Masonic, K.; Heiffer, M. H.; Brewer, T. G. *J. Pharm. Pharmacol.* **1998**, *50*, 173–182.

(9) Pathak, A. K.; Jain, D. C.; Sharma, R. P. *Indian J. Chem., Sect. B: Org. Chem. Incl. Med. Chem.* **1995**, *34*, 992–993.

(10) Haynes, R. K.; Chan, H. W.; Cheung, M. K.; Chung, S. T.; Lam, W. L.; Tsang, H. W.; Voerste, A.; Williams, I. D. *Eur. J. Org. Chem.* **2003**, 2098–2114.

(11) Luo, X.; Yeh, H. J. C.; Brossi, A.; Flippen-Anderson, J. L.; Gilardi, R. *Helv. Chim. Acta* **1984**, *67*, 1515–1522.

(12) Haynes, R. K.; Chan, H. W.; Cheung, M. K.; Lam, W. L.; Soo, M. K.; Tsang, H. W.; Voerste, A.; Williams, I. D. *Eur. J. Org. Chem.* **2002**, 113–132.

(13) Haynes, R. K. *Curr. Topics Med. Chem.* **2006**, *6*, 509–537.

(14) Navaratnam, V.; Mordi, M. N.; Mansor, S. M. *J. Chromatogr. B* **1997**, *692*, 157–162.

(15) Batty, K. T.; Davies, T. M. E.; Thu, L. T.; Binh, T. Q.; Anh, T. K.; Ilett, K. F. *J. Chromatogr. B* **1996**, *677*, 345–350.

(16) Batty, K. T.; Ilett, K. F.; Davis, T. M. E. *J. Pharm. Pharmacol.* **1996**, *48*, 22–26.

(17) Batty, K. T.; Ilett, K. F.; Davis, T. M. E. *Br. J. Clin. Pharmacol.* **2004**, *57*, 529–533.

(18) Maggs, J. L.; Madden, S.; Bishop, L. P.; O'Neill, P. M.; Park, K. B. *Drug Metab. Dispos.* **1997**, *25*, 1200–1204.

(19) Ramu, K.; Baker, J. K. *J. Med. Chem.* **1995**, *38*, 1911–1921.

(20) (a) Angelini, G.; Chiappe, C.; De Maria, P.; Fontana, A.; Gasparrini, F.; Pieraccini, D.; Pierini, M.; Siani, G. *J. Org. Chem.* **2005**, *70*, 8193–8196.(b) Schneider, H. J.; Yatsimirsky, A. *Principles and Methods in Supramolecular Chemistry*; John Wiley & Sons Ltd.: Chichester, 1999; pp 119−135.

(21) (a) ACD/Labs Package V. 6.00, (pKa DB Module), 90 Adelaide Street West Toronto, Ontario M5H 3V9, Canada. (b) Marvin 4.1.1.3, 2007, ChemAxon (http://www.chemaxon.com). These packages were used to draw and calculate pK_a values of hemiacetalic structures.

(22) (a) Fontana, A.; De Maria, P.; Siani, G.; Pierini, M.; Cerritelli, S.; Ballini, R. *Eur. J. Org. Chem.* **2000**, 1641–1646. (b) Angelini, G.; De Maria, P.; Fontana, A.; Pierini, M.; Siani, G. *J. Org. Chem.* **2007**, *72*, 4039–4047. (c) Cirilli, R.; Costi, R.; Di Santo, R.; Gasparrini, F.; La Torre, F.; Pierini, M.; Siani, G. *Chirality* **2009**, *21*, 24–34.

(23) (a) McClelland, R. A.; Kanagasabapathy, V. M.; Mathivanan, N. *Can. J. Chem.* **1991**, *69*, 2084–2093. (b) Sorensen, P. E.; Jencks, W. P. *J. Am. Chem. Soc.* **1987**, *109*, 4675–4690.

(24) The chemical shift of the hydroxyl hydrogen is directly correlated to its ability to form an H-bond with the solvent. Therefore, the chemical shift of such protons for both isomers is more deshielded in d_6-DMSO (6.37 and 6.23 ppm for α and β, respectively) than in CD_3CN (4.23 and 4.07 ppm). Furthermore, in both of these solvents the trend was the same, the α-epimer being more deshielded than the β one. This behavior agrees with the calculations, which predicted the α-hydroxyl to be more acidic than the β one.

(25) (a) Keller, R. A.; Giddings, J. C. *J. Chromatogr.* **1960**, *3*, 205–220. (b) Kramer, R. *J. Chromatogr.* **1975**, *107*, 241–252. (c) Schurig, V.; Bürkle, W. *J. Am. Chem. Soc.* **1982**, *104*, 7573–7580. (d) Bürkle, W.; Karfunkel, H.; Schurig, V. *J. Chromatogr.* **1984**, *288*, 1–14. (e) Veciana, J.; Crespo, M. I. *Angew. Chem., Int. Ed. Engl.* **1991**, *30*, 74–77. (f) Jung, M. *QCPE Bull.* **1992**, *12*, 52. (g) Cabrera, K.; Jung, M.; Fluck, M.; Schurig, V. *J. Chromatogr. A* **1996**, *731*, 315–321. (h) Oxelbark, J.; Allenmark, S. *J. Org. Chem.* **1999**, *64*, 1483–1486. (i) Trapp, O.; Schoetz, G.; Schurig, V. *Chirality* **2001**, *13*, 403–414. (j) Wolf, C. *Chem. Soc. Rev.* **2005**, *34*, 595–608. (k) Trapp, O. *Anal. Chem.* **2006**, *78*, 189–198. (l) D'Acquarica, I.; Gasparrini, F.; Pierini, M.; Villani, C.; Zappia, G. *J. Sep. Sci.* **2006**, *29*, 1508–1516.

(26) (a) Gasparrini, F.; Lunazzi, L.; Mazzanti, A.; Pierini, M.; Pietrusiewicz, K. M.; Villani, C. *J. Am. Chem. Soc.* **2000**, *122*, 4776–4780. (b) Dell'Erba, C.; Gasparrini, F.; Grilli, S.; Lunazzi, L.; Mazzanti, A.; Novi, M.; Pierini, M.; Tavani, C.; Villani, C. *J. Org. Chem.* **2002**, *67*, 1663–1668. (c) Gasparrini, F.; Grilli, S.; Leardini, R.; Lunazzi, L.; Mazzanti, A.; Nanni, D.; Pierini, M.; Pinamonti, M. *J. Org. Chem.* **2002**, *67*, 3089–3095. (d) Dalla Cort, A.; Gasparrini, F.; Lunazzi, L.; Mandolini, L.; Mazzanti, A.; Pasquini, C.; Pierini, M.; Rompietti, R.; Schiaffino, L. *J. Org. Chem.* **2005**, *70*, 8877–8883. (e) Cirilli, R.; Ferretti, R.; La Torre, F.; Secci, D.; Bolasco, A.; Carradori, S.; Pierini, M. *J. Chromatogr. A* **2007**, *1172*, 160–169.

(27) Cabri, W.; Ciogli, A.; D'Acquarica, I.; Di Mattia, M.; Galletti, B.; Gasparrini, F.; Giorgi, F.; Lalli, S.; Pierini, M.; Simone, P. *J. Chromatogr. B* **2008**, *875*, 180–191.

(28) (a) Stott, K.; Stonehouse, J.; Keeler, J.; Hwand, T.-L.; Shaka, A. J. *J. Am. Chem. Soc.* **1995**, *117*, 4199–4200. (b) Stott, K.; Keeler, J.; Van, Q. N.; Shaka, A. J. *J. Magn. Reson.* **1997**, *125*, 302–324. (c) Van, Q. N.; Smith, E. M.; Shaka, A. J. *J. Magn. Reson.* **1999**, *141*, 191–194.